Anomalous Behavior of the Atmospheric Surface Layer over a Melting Snowpack

ISIDORE HALBERSTAM[1] AND JOHN P. SCHIELDGE

Jet Propulsion Laboratory, Pasadena, CA 91103

(Manuscript received 16 June 1980, in final form 13 October 1980)

ABSTRACT

During March, 1978 on a snow-covered field near Lee Vining, California, measurements were made that included: 1) variations above the snow surface of the net radiative flux and the profile of wind speed, air temperature and relative humidity; and 2) variations beneath the snow surface of the conductive heat flux and the temperature profile. The period was marked by clear skies, warm air and calm winds during the day, and cold air and moderate winds at night. During the day, a highly stable sublayer formed near the surface, with a persistent warm layer at ~0.5 m above the surface. At night, profiles agreed more with classical log-linear forms found in stable air. Numerical simulation of long and shortwave radiative fluxes near the surface, using observed humidity profiles, produced the daytime warm level in agreement with observations. It was concluded that in the absence of turbulent mixing, strong solar radiation and a supply of moisture from the snow will cause a raised maximum of temperature during the day.

1. Introduction

During the winter, much of the Northern Hemisphere is snow covered and significant portions remain under snow even during the warm months. Snow, however, is not a passive product of weather conditions but an active participant in the creation of air masses (Wexler, 1936) and seasonal fluctuations (Kukla and Kukla, 1974). The interaction of the snow with the atmosphere covers a wide range of phenomena, including the radiative, conductive, and convective fluxes at the surface. To understand these interactions, a program of measurement, analysis, and modeling must be undertaken. In fact, because of the difficulties involved in obtaining accurate measurements over snow, little progress has been made in understanding the atmospheric response to snow surfaces.

Recently, numerical models (Anderson, 1976; Halberstam and Melendez, 1979) and field experiments (De La Casaniere, 1974; McKay and Thurtell, 1978; Granger, 1977; Granger and Male, 1978) have shed some light on various aspects of air-snow interactions. All investigators, however, have had difficulties in estimating the net energy flux at the surface. This arises because the turbulent transport of energy is damped in stable air, and the air in the surface layer above a snowpack is believed to be generally stable. Stability is induced from below by the cold snow surface where temperatures are restricted to remain at or below 0°C. Furthermore, the surface temperature is altered by volumetric and surface changes in the physical properties of the snow, *viz.*, density, heat capacity and conductivity, albedo and solar opacity. These changes occur rapidly during a thaw when warm air is advected over a snowpack.

In general, hydrologists have been concerned about changes in the snow caused by daily to seasonal atmospheric variations. Meteorologists, on the other hand, should be concerned with the complementary influences of snow on air in the surface layer, especially during thaw periods when the snow is undergoing rapid change.

It was for this purpose that an experiment was conducted at Lee Vining, California, during a warm period in March 1978. The goal of the experiment was to obtain detailed profile measurements of meteorological variables in the atmosphere directly above a snow surface and to monitor the radiative and conductive fluxes at the surface. These should furnish a detailed quantitative description of the changing fluxes across the air-snow interface. The experiment was conducted for only 3.5 days because of increasing danger of slippage to the experiment. During that brief time, however, the nearly steady-state weather conditions were fairly typical of a spring thaw.

2. Description of the experiment

The site selected for the measurements is a snow-covered field located just south of Lee Vining, CA, a small town at the east entrance of Yosemite National Park which contains a portion of the Sierra-

[1] Current affiliation: Systems and Applied Sciences Corp., Lexington, MA.

0021-8952/81/030255-11$06.75

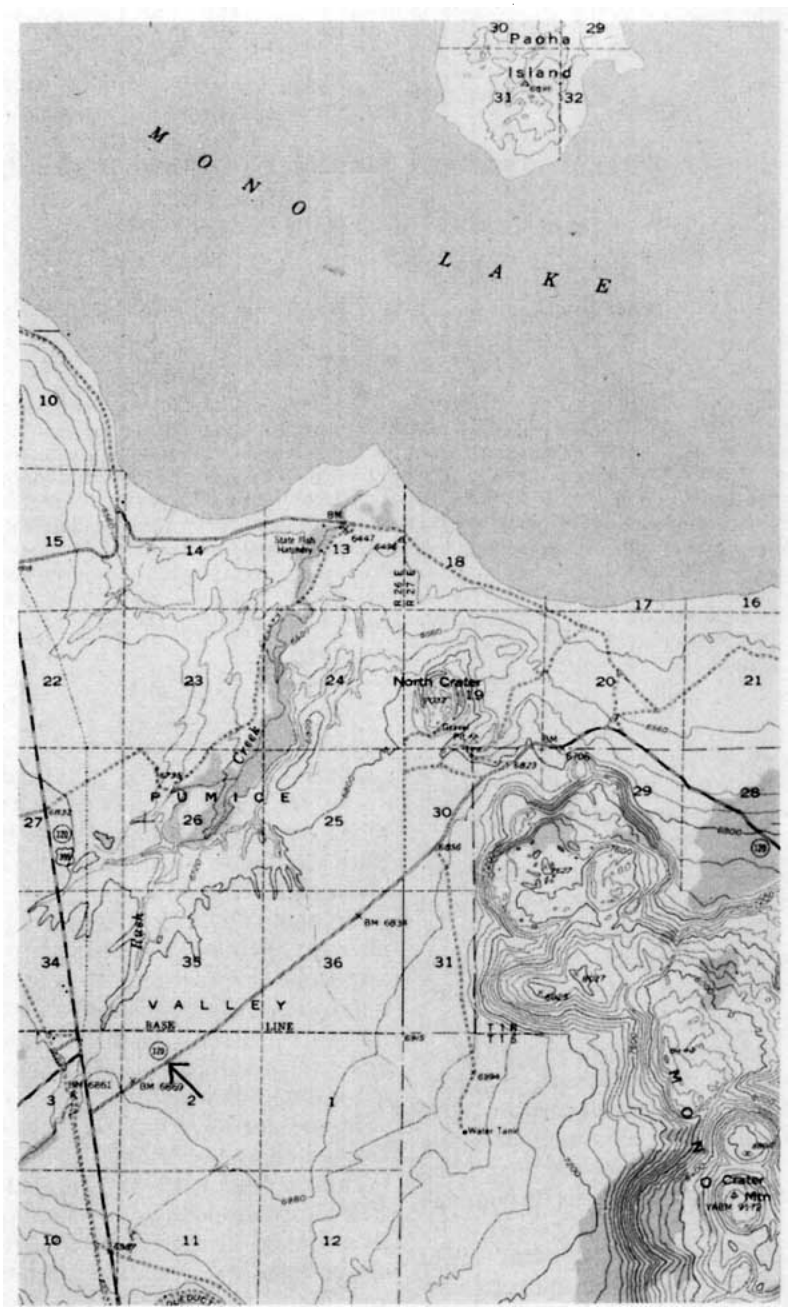

FIG. 1. Topographical map of site (marked by arrow) area. Contours are labeled in feet.

Nevada Range. The field's elevation is approximately 2100 m above msl and is fairly uniform in all directions for ~4 km. Beyond that distance to the west, the foothills of the Sierras begin. The field is fairly smooth to the south for 8 km while at ~5 km east of the site, Mono Craters rise to some 90 m above the field. The lake remains ice-free all winter. A relief map of the area is shown in Fig. 1; the site is located just below the Mt. Diablo base line at the point where the circled road marker 120 appears.

Atmospheric profile measurements were made by cup anemometers, thermistor thermometers, and lithium-chloride dew-point sensors that were mounted over the snow surface on an 8 m mast. The instruments were supported on booms, spaced logarithmically at ⅛, ¼, ½, 1, 2, 4 and 8 m (Kahle *et al.*, 1977). One anemometer was placed at each level while the dew point sensors were placed only at ½, 1 and 2 m. There were two thermistors at every level except where the dew point sensors took the place

of one thermistor. All these were connected to an automated recorder which took 960 s (16 min) averages of temperature, humidity and wind speeds. Some problems with the electronics occurred in recording the data. Data were not always obtained at all levels at all times. In particular, the temperature at 1 m was recorded intermittently. Nonetheless, most data sets consisted of at least five levels of information. For comparison, a portable weather station manufactured by Meteorology Research, Inc. (MRI) was installed about 20 m southeast of the profile equipment. The MRI was used to monitor wind direction and to provide an initial calibration for the wind speed, temperature and humidity. Net radiation was measured at 0.5 m by a Thornthwaite Model 602 net radiometer. It consisted of a flat, circular black plate (thermal transducer) shielded by two clear plastic hemispheres. A Thornthwaite soil heat flux sensor was placed just beneath the snow surface to measure conductive flux through the snow. The sensor is a thin plate across which temperature differences are related to heat transfer. The net radiation and soil heat flux sensors were each connected to a strip chart recorder.

The period of the experiment from 15–19 March 1978 was marked by a warming trend over most of the western third of the U.S. National Weather Service (NWS) analyses of the surface and 50 kPa are portrayed in Figs. 2a and b for 1200 GMT 18 March. The large, stationary ridge covering the West was responsible for near-record temperatures in central and southern California.

Weather conditions at the site were nearly uniform throughout: clear skies and low humidity prevailed until 18 March. After that, cirriform clouds caused sky conditions to vary from broken to overcast.

3. Analysis of measurements

The profiles of temperature, wind and humidity were often anomalous compared with classical logarithmic forms. Due to a combination of light winds and a cold surface, the atmosphere near the ground usually separated into distinct thermal layers, especially during the day. During the early evening, winds increased due either to a channeling effect from the surrounding mountains, or to a thermally induced circulation near Mono Lake. When the winds increased, the anomalies disappeared and the profiles assumed the quasi-logarithmic forms that are typical of well-mixed turbulent layers.

Figs. 3 and 4 show the wind and temperature records at the 8 and 0.25 m level. Both rise and fall in irregular patterns throughout the period. The temperature record indicates nearly isothermal conditions during most of the day, with rapid cooling at the surface soon after sunset (~1700 LT). Unstable conditions are seen to occur around the noon hour, a surprising result which will be discussed in greater detail below.

Figs. 5a–5d and 6a–6d show the development of the temperature (upper scale), wind speed (lower scale), and specific humidity profiles for 0747, 1153, 1329 and 1521 LT on 18 March. The temperature profiles exhibit an elevated maximum at about 0.5 m throughout the day. At midday, temperatures at that level approach 14°C. Such behavior is expected over blacktop surfaces on clear summer days rather than snow surfaces. The profile below the maximum, on the other hand, is very stable falling to the presumed 0°C surface temperature from 14°C in just 0.5 m. The humidity profiles show that sublimation is taking place during the day, doubling the early morning readings by midday. Here again, there is a sharp gradient in the lowest 0.5 m during midday, where the specific humidity increases from about 4.5×10^{-3} to the assumed saturated surface value of 5.067×10^{-3}. Near sunset the exaggerated gradients disappear for both temperature and humidity. During the day, the winds blew from the south or southeast for the most part; however, this regime was interrupted briefly by periods (~1 h) when the wind direction was variable.

When profiles are logarithmic, with some deviations due to stability, turbulent heat fluxes at the surface can be calculated by Paulson's (1970) method. First, a bulk Richardson number Ri_B is obtained from the profiles (Lettau, 1957); next, the Monin-Obukhov scale length L is calculated by inserting Ri_B in the empirical formulas of say, Businger *et al.* (1971); finally, the integrated forms of the Businger relations are expressed as functions of L and the profile data are fit to them by least squares. From this analysis, the surface roughness length z_0 and the turbulent heat fluxes are obtained. This method, however, can not be applied to the irregular profiles illustrated in Figs. 5 and 6.

Instead, we estimate the turbulent heat fluxes indirectly. At the one-dimensional air-snow interface, a balance exists according to the relations

$$Q_L\uparrow + Q_L\downarrow + Q_E + Q_S + Q_C = 0, \qquad (1)$$

where $Q_L\uparrow$ and $Q_L\downarrow$ are the longwave outgoing and incoming radiation, respectively, Q_E the latent heat flux, Q_S the sensible heat flux, and Q_C the conductive heat flux in the snow. The solar heat flux is not included in this expression because the snow surface is translucent. Instead, solar radiation penetrates the snow surface and acts as an internal source rather than a surface flux, as explained by Halberstam and Melendez (1979). This internal source then contributes to the conductive heat flux and the outgoing longwave radiation. The net radiometer used in this experiment included solar radiation, measured at 0.5 m. The soil flux meter placed right below the snow surface was also sensitive to the solar flux

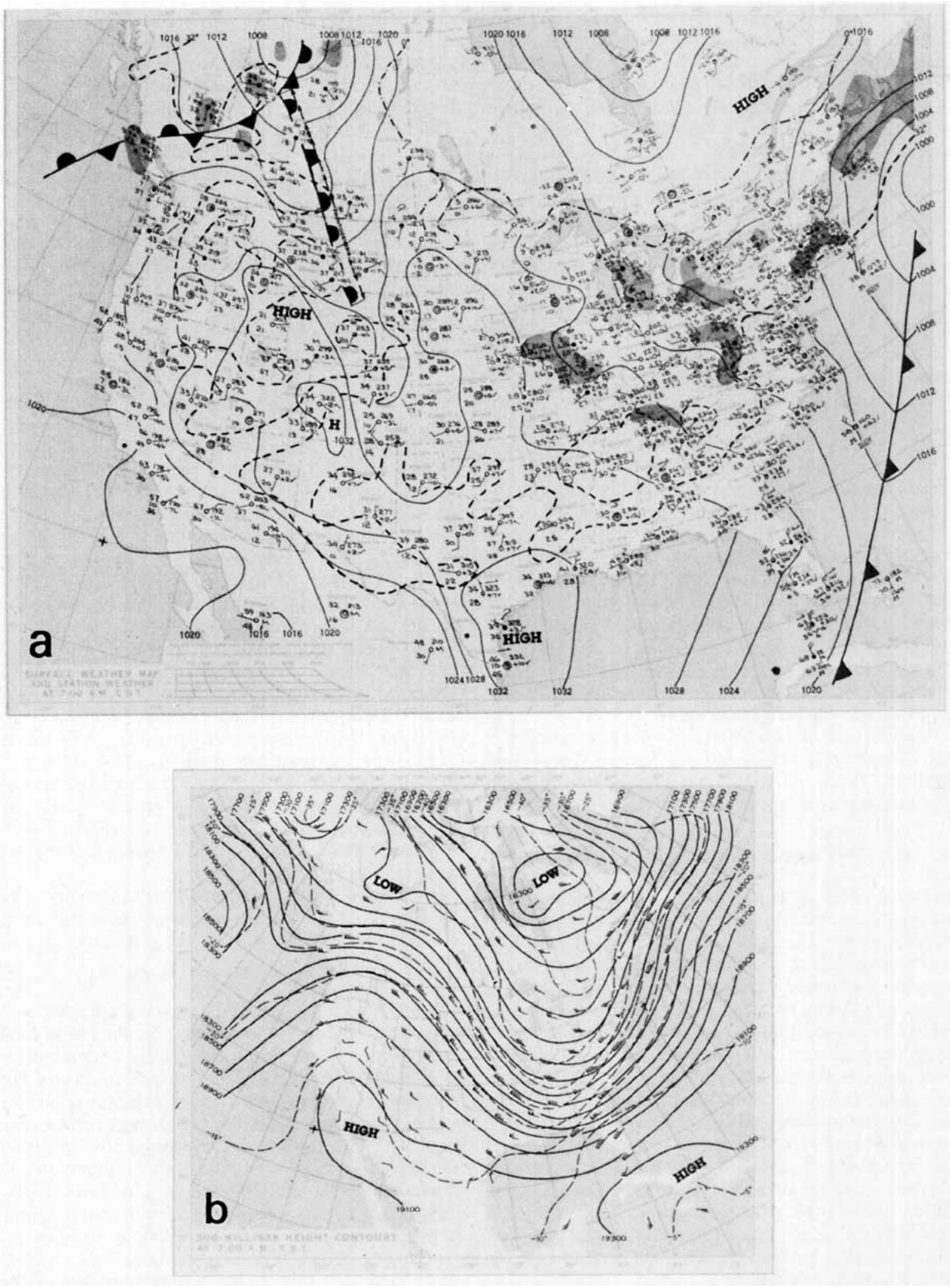

FIG. 2. NWS analysis of (a) surface and (b) 50 kPa level maps at 1200 GMT on 18 March 1978.

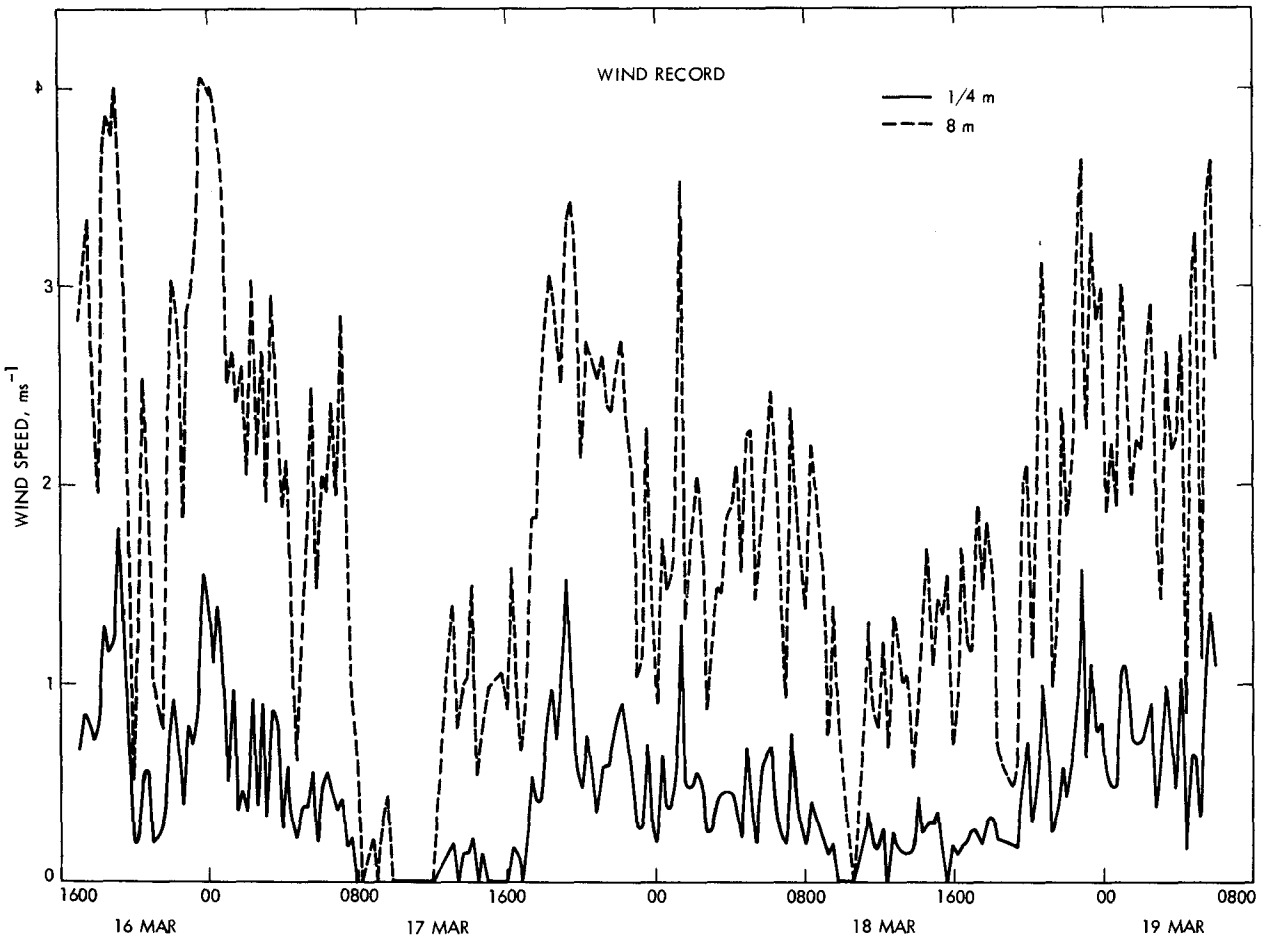

FIG. 3. Wind record from mast for the 8 m (broken line) and ¼ m (solid line) levels from 1600 PST 16 March to 0800 PST 19 March 1978.

passing through the snow and effectively can be used to subtract the solar influence. Of course it would have made more sense to measure each flux separately, but not all the necessary equipment was available at the time of the experiment. Another problem involved in this comparison stems from measuring the net radiation at 0.5 m rather than directly at the surface. The warm layer at 0.5 m indicates that the radiative flux may vary considerably near the surface so that measurements anywhere but directly at the surface may not be representative of the actual surface fluxes. With these considerations in mind, one may analyze the net radiation, conduction and their sum depicted in Fig. 7. The period shown is only from noon on 16 March to 0900 on 19 March when both instruments were functioning. There is a gap on the afternoon of the 17th because of a malfunction in the net radiometer, but that was corrected later that night. The sum of the radiative and conductive fluxes should be close to the sum of the turbulent fluxes. Again, the estimate here is probably better at night, but daytime measurements can furnish approximate values for the fluxes. As can be seen, the sum barely reaches 100 W m^{-2}, with daytime values peaking usually at ~60 W m^{-2}.

Profiles of temperature in the snow probably indicate melting during the day and refreezing at night. Fig. 8 shows the changing profiles from the morning of 16 March until the morning of 17 March. During the night, the temperatures cool off rapidly causing the upper portion of the snow to become cold. The snow below 30 cm remains fairly insulated throughout the night. Toward morning, the surface temperature reaches a minimum temperature, but then it rapidly rises in response to solar insolation. The melt process helps create an almost isothermal snowpack not only at noon but also for some time thereafter.

4. Discussion

The observed surface layer behavior requires careful analysis. The anomalous profiles and the erratic temperature and wind record are not unique to

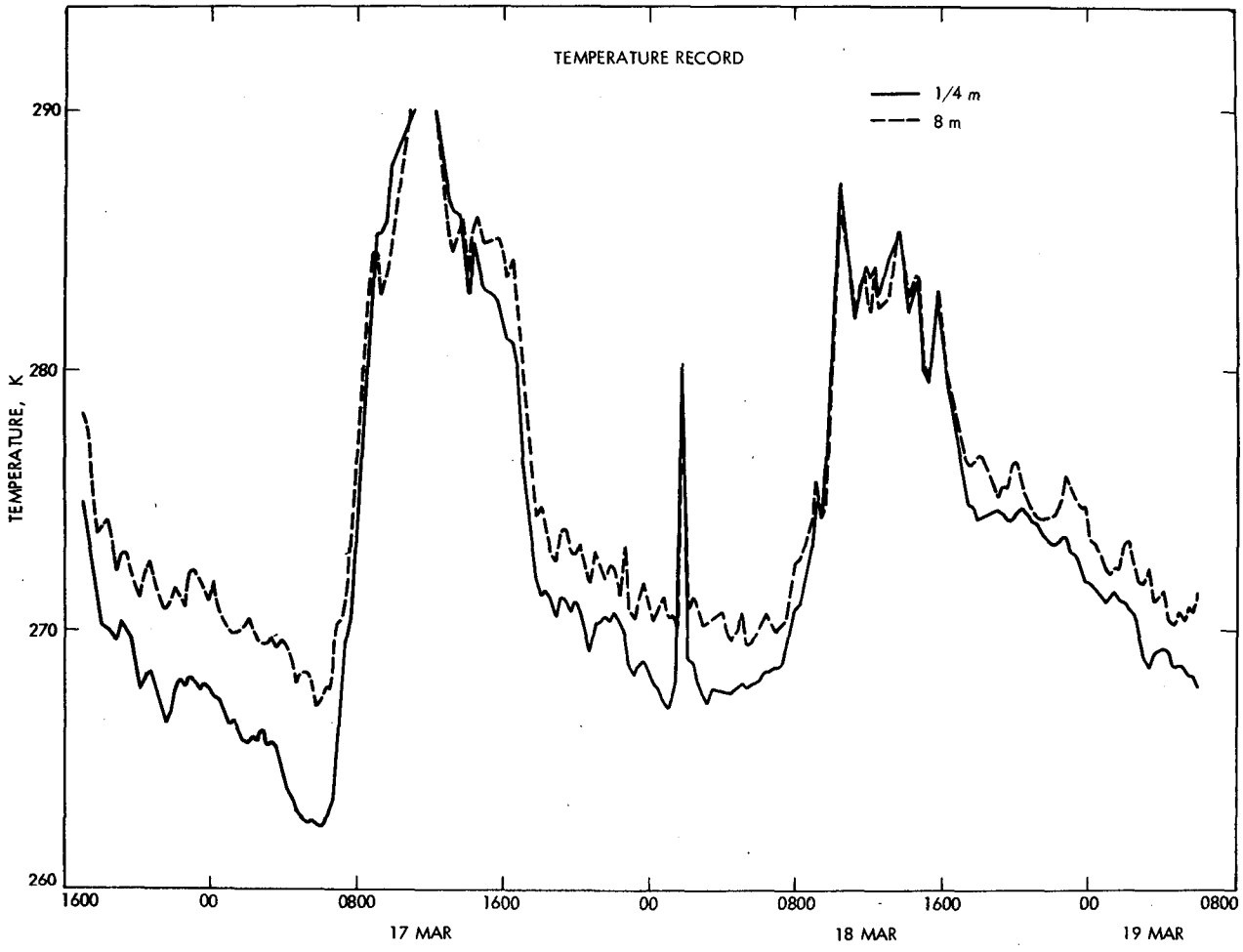

FIG. 4. As in Fig. 3, except for temperature.

this experiment but are surely exaggerated by the snow cover and the light winds. Both of these factors tend to increase stability so much that turbulent motions are rapidly damped in the surface layer. When this happens, first-order turbulence models, such as the Businger relations, are incapable of describing the weak and irregular exchange processes.

Furthermore, the sporadic rising and falling of temperatures and winds in Figs. 3 and 4 may be related to the "burst" phenomenon described by Businger (1973) and observed by Schubert (1977). It is caused by strong radiative cooling, especially at night, which damps turbulent motion, creating a laminar layer atop a shallow turbulent layer. As turbulent motions are damped by the combination of increasing buoyancy and surface friction, the shear between the turbulent and laminar zones is increased. When the shear becomes so great as to reduce the Richardson number to below critical value ($Ri < 0.21$), a burst of warm air is brought to the surface and the cycle begun anew. The time scale associated with these bursts is variable, so that a 16 min average may not be truly representative.

More difficult to explain is the layering during the day in the first meter above the snow. One would expect when the surface temperature is significantly colder than the air, that an intense stable sublayer would form immediately above the surface. Above that, the air should be fairly isothermal (or adiabatic). Why a raised maximum should persist at 0.5 m is not clear. Skibin (1976) observed frequent layering in stable surface layers, but that was probably due to the burst process in its various stages; no evidence was presented of a persistent sublayer. De La Casaniere (1974) and Granger and Male (1978) reported similar layering near snow surfaces, but not of the magnitude recorded here. De La Casaniere blamed this behavior on surface roughness effects not adequately accounted for by z_0 and "intense absorption of the infrared by the water vapor in the air." He begins his flux calculations above the sublayer, where similar to our findings, the profiles

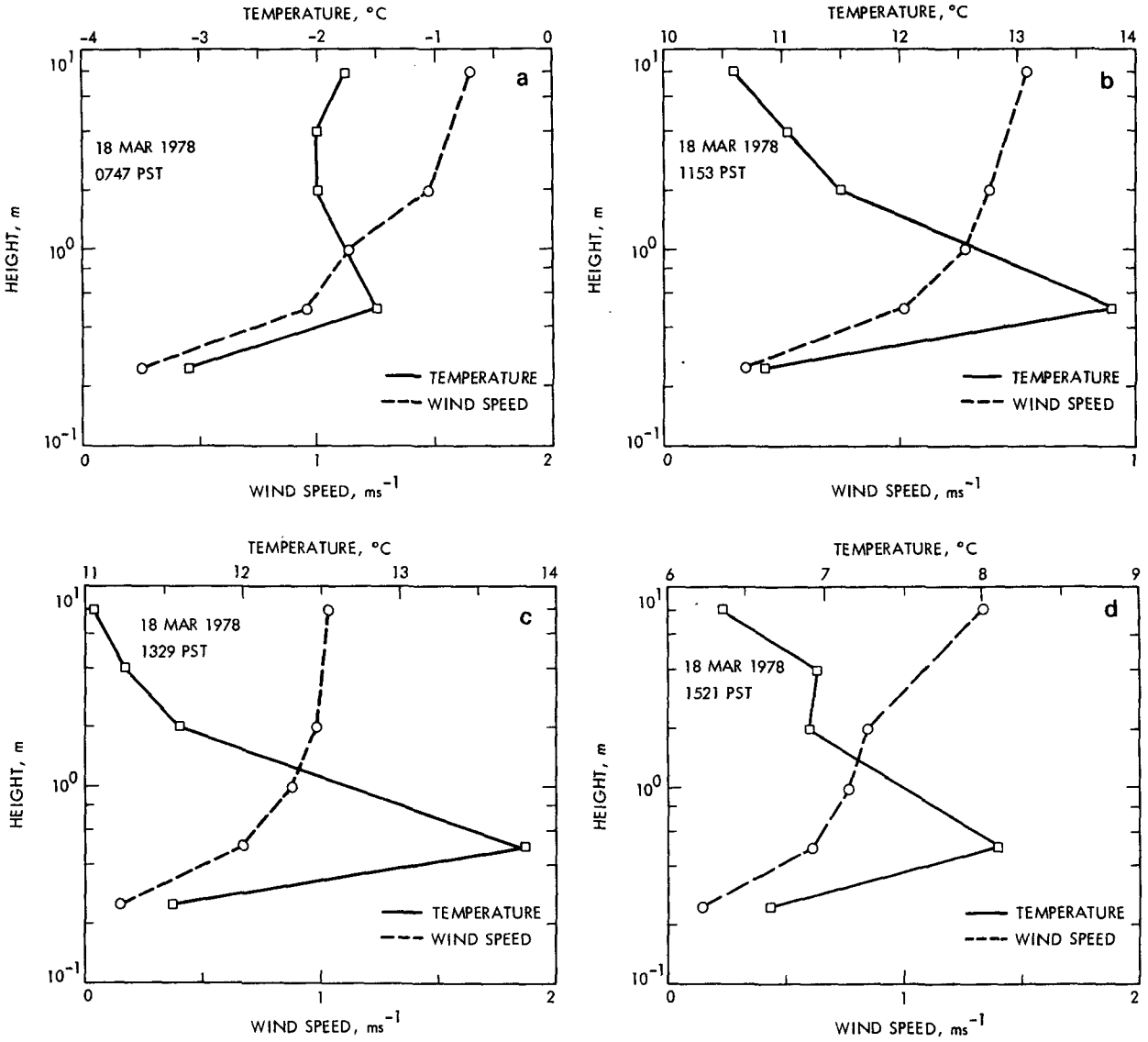

FIG. 5. Wind (lower scale) and temperature (upper scale) profiles from mast for (a) 0747, (b) 1153, (c) 1329 and (d) 1521 PST on 18 March. (Differences in time increments between measurements are not always integral multiples of 16 min because maintenance duties required starting and stopping the equipment at arbitrary times.)

show more orthodox form. Granger and Male do not discuss the warm layer in their published report, but Granger (1977) briefly mentions that such warming could be the result of "radiative flux divergence." The question is why should such divergence (or convergence) exist in the lowest layer? One is tempted to ask whether there is a parallel between this raised maximum and the observed nighttime raised minimum. This phenomenon has been reported by many investigators, as mentioned by Geiger (1965), and verified by Oke (1970), who suggested that longwave radiative flux divergence, aided by a discontinuous humidity profile, caused a loss of heat from an elevated layer. Zdunkowski (1966) attempted to model the raised minimum, but found that long-wave radiative emission from a layer of water vapor is insufficient to account for it. Instead, he suggested that a haze or fog layer could act as strong radiators, cooling a level above the surface. In our case, they could not explain the raised maximum, because, first we did not observe any fog or haze (except for a very thin layer right before daybreak on 18 March) and, second, the raised maximum persisted well into the afternoon, when the fog or haze would surely have evaporated. The humidity, however, did increase with decreasing height suggesting there may be a connection between the humidity and temperature behavior.

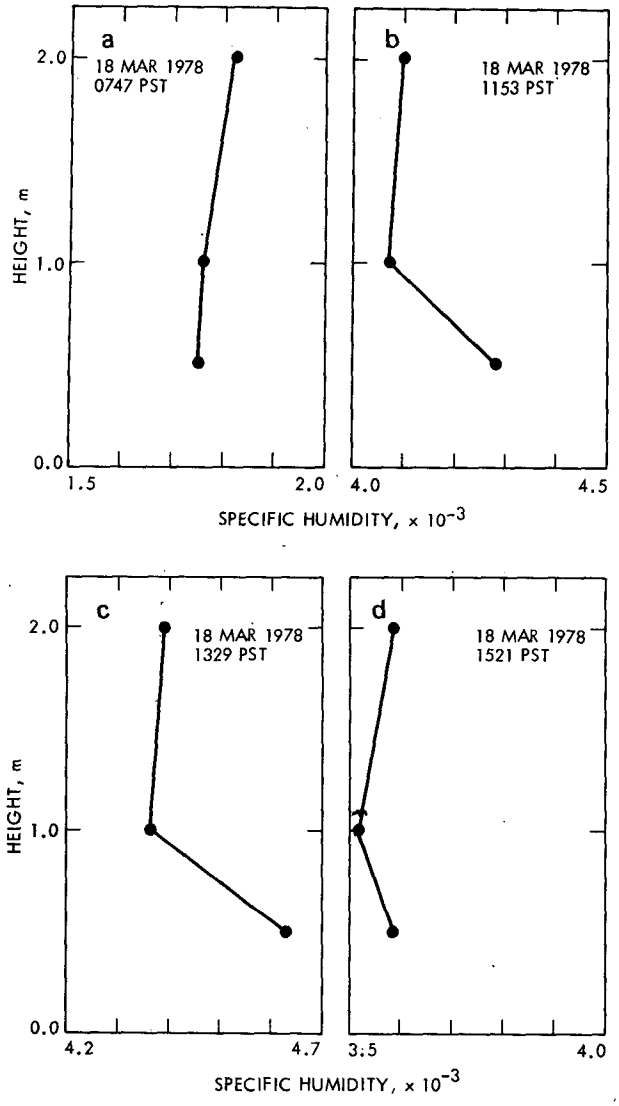

FIG. 6. As in Fig. 5 except for specific humidity.

To see if indeed the observed humidity profile could produce the longwave radiative flux divergence necessary for the raised maximum, we estimated the temperature change in air due to radiative divergence with a numerical model. Using the humidity data from 1357 LT 17 March at 0.5, 1 and 2 m, we calculated the steady-state temperature profile at those levels due to longwave flux divergence, using Kondrat'yev's (1968) formula for temperature change:

$$\frac{\partial T}{\partial t} = q\left[\int_{P_0}^{P}\frac{\partial \tau}{\partial \omega}\frac{\partial B}{\partial P}\,dP - B_\infty\left(\frac{\partial \tau}{\partial \omega}\right)_\infty - \int_{P}^{P_T}\frac{\partial \tau}{\partial \omega}\frac{\partial B}{\partial P}\,dP\right]C_P^{-1}, \quad (2)$$

where C_P is the heat capacity of air, B is the Planck function, τ is the transmission function, ω is the precipitable water vapor, P is atmospheric pressure at the level in question, and P_T is an arbitrary pressure at the top of the atmosphere. The function τ is given as the sum of four wavelength bands

$$\tau = \tfrac{1}{4}\sum_{i=1}^{4} e^{-k_i\omega}, \quad (3)$$

where k_i are absorption constants for water vapor at distinct wavelength bands.

For atmospheric pressures, we used $P_T = 30$ kPa and $P_0 = 75$ kPa. The first term in (2) was integrated numerically from P ($z = 0$) to P ($z = 2$ m) using observed and calculated values of q and T. Next, by assuming a relationship $T/T_0 = (P/P_0)^\gamma$ and $q/q_0 = (P/P_0)^a$ for $z = 2$ m, we evaluated the second and third terms. The third term becomes

$$-\sigma\gamma T_0^4 P_0^{-4\gamma}\int_P^{P_T}\sum_{i=1}^{4} k_i \times \exp\left\{k_i\left[\frac{q_0}{(a+1)g}\left(\frac{P^{a+1}}{P_0^a} - P_0\right) + \mu\right]\right\}P^{4\gamma-1}dp,$$

where μ is ω at P and σ is the Stefan-Bolzmann constant. The integral above is not analytically soluble unless $4\gamma - 1 = a$. For adiabatic conditions $4\gamma - 1 \approx 0.1$, while a is normally chosen >1. Expansion of the exponential in terms of a series is not practical because of the large arguments. Instead, it is possible to write $P^{4\gamma-1} = P^a P^{4\gamma-1-a}$, and remove a mean $\bar{P}^{(4\gamma-1-a)}$ from the integral. The integral, then, becomes equal to

$$\frac{-\sigma g\gamma T_0^4 P_0^{a-4\gamma}}{q_0\bar{P}^{(a+1-4\gamma)}}\sum_{i=1}^{4}\exp\{-k_i[q_0P_0(a+1)^{-1}g^{-1} - \mu]\} \times \{\exp[\alpha_i P_T^{(a+1)}] - \exp[\alpha_i P_0^{(a+1)}]\};$$

where $\alpha_i = k_i q_0[(a+1)gP_0^a]^{-1}$. The integral need only be evaluated once, the only time variable being T_0, the temperature at 2 m.

Eq. (2) was solved numerically with fixed humidity and surface temperature (0°C). A 10 min time step was used. Two cases were tested: the first with $a = 2.0$ and $\gamma = 0.286$ (adiabatic); the second with $a = 1.2$ and $\gamma = 0.20$. In both cases, equilibrium ($\partial T/\partial t < 10^{-7}$ °C s^{-1}) was reached at near isothermal conditions (see Table 1). Thus, although the humidity profile may slightly affect the equilibrium temperatures, they do not exhibit the observed local maximum.

The only source of atmospheric heating in the absence of strong winds is solar radiation. Although shortwave radiative flux divergence in the lower atmosphere is generally considered negligible [although Faraponova *et al.* (1968) showed that this is not the case], an exception can be made for the present situation. First, the atmosphere is humid near the snow but quite dry aloft. Second, the elevation of

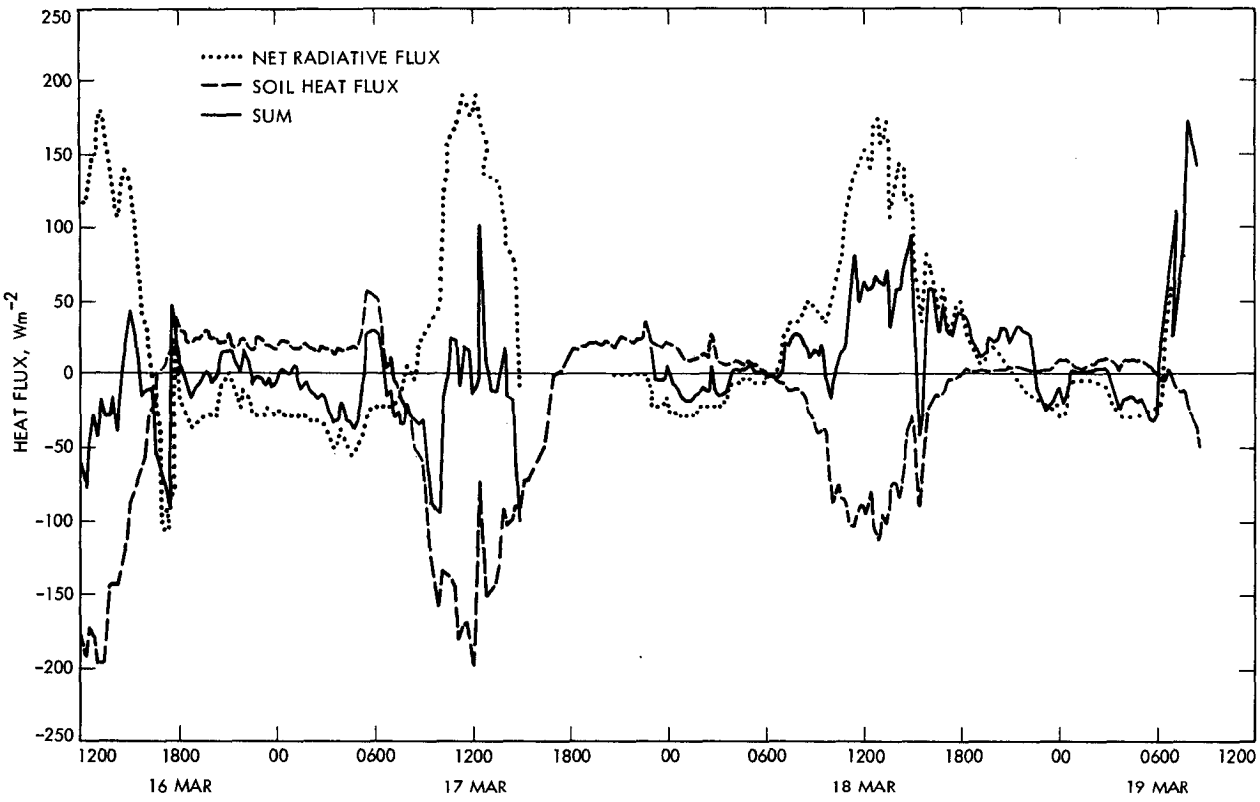

FIG. 7. Net radiative (dotted line), conductive soil (broken line), and inferred turbulent heat fluxes from measurements with the net radiometer and soil heat flux meter. (The conductive "soil" flux variation pertains to measurements made within the snow pack.)

the site resulted in intense solar radiation. Third, the high albedo of snow almost doubles solar radiation in the air near the surface.

We added the effect of solar radiation to the longwave calculations by employing the following relations for F_s, the solar flux at any level

$$F_s = S_0 \cos\hat{Z}(1 - \beta), \tag{4}$$

where S_0 is the solar constant, $\hat{Z}$ the solar zenith angle and β the absorptivity of the column directly above the level in question. The equation for β was taken from Washington and Williamson (1977)

$$\beta = 0.11(\omega \sec\hat{Z} + 6.31 \times 10^{-4})^{0.3} - 0.0121. \tag{5}$$

$\hat{Z}$ is a function of solar declination δ, latitude ϕ and hour angle h. Since observations in our case were made very close to the equinox (i.e., $\delta \approx 0$, the expression for $\hat{Z}$ reduced to

$$\cos\hat{Z} = (\cos\phi)(\cos h). \tag{6}$$

It was thus possible to compute fluxes at any level and the temperature changes due to the sum of solar and longwave radiation for a diurnal cycle. We assumed a value of $S_0 = 900$ W m^{-2} (to take into account scattering and absorption by other gases) and a fixed ground temperature of 0°C. Fig. 9 shows the temperatures calculated at 0.5, 1, and 2 m for a

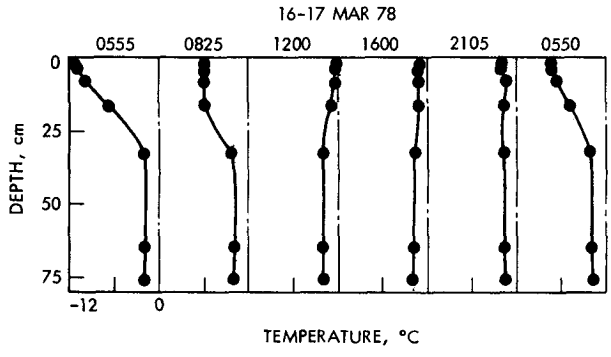

FIG. 8. Variations in the snow temperature profile from the morning of 16 March to the morning of 17 March. The temperature range for all panels is from −12 to 0°C.

TABLE 1. Equilibrium temperatures from Eq. (2) at three heights above the snow surface, assuming two different temperature and humidity profiles above 2 m.

Height (m)	$a = 2.0$, $\gamma = 0.286$	$a = 1.2$, $\gamma = 0.20$
½	272.07	272.45
1	272.06	272.44
2	272.05	272.44

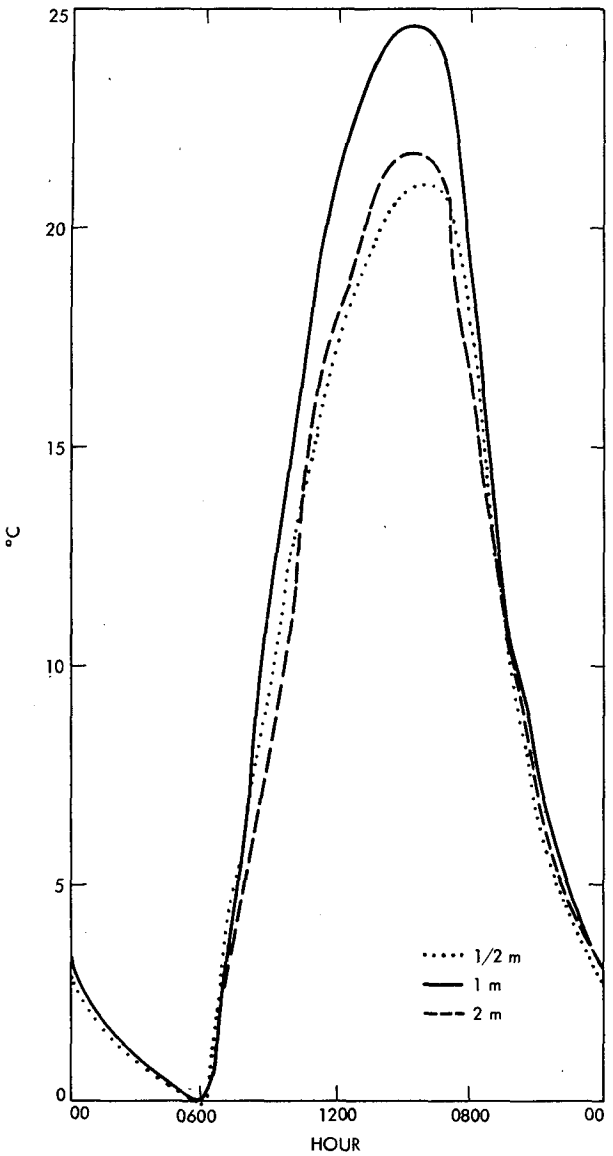

FIG. 9. Computed air temperature at ½ (dotted line), 1 (solid line) and 2 m (broken line) using a joint longwave and shortwave radiative flux model.

full cycle, showing clearly a raised maximum during daylight at 1 m and a large temperature difference between the snow surface and the air. At night, the temperatures are nearly isothermal, because surface cooling was omitted from the calculations. It is apparent that solar radiation, combined with a humid layer, is a major contributor to the raised maximum during the day. The full mechanism of its development will be summarized below.

5. Summary and conclusions

Atmospheric and related snowpack data have been measured for a flat snowfield during warm, clear and mostly calm conditions. The profiles of temperature, winds, and humidity were examined and turbulent fluxes were estimated from the sum of radiative and conductive fluxes at the snow surface.

In the present experiment, as well as in other similar experiments over snow, a persistent daytime warm layer is found at about 0.5 m above the surface. The warm layer is apparently a product of light winds, strong solar radiation, and the presence of a snow surface. As the sun shines on the snow surface, some of the snow sublimates into the atmosphere. Because of high stability and low wind speeds, the water vapor does not diffuse to high levels but remains concentrated in the lower surface layer. Because of the dry upper atmosphere and the elevation of the site, much of the solar radiation that is normally absorbed en route by water vapor reaches the surface layer. The lowest levels then absorb solar radiation in both directions (downward and reflected upward) with the more humid atmosphere near the surface absorbing most of the solar energy. the layers of water vapor nearest the surface lose their heat because of longwave radiative emission and weak turbulent mixing. The upper levels also lose more heat than the middle layers due to less absorption of solar radiation and more longwave radiation to space.

As soon as the sun sets, the process abruptly ends. The snow surface cools rapidly, sublimation ceases, and the atmosphere no longer receives heat from the sun. A stable profile is formed in the surface layer interrupted by periodic bursts from the overlying laminar layer. When winds increase, Ri drops below 0.21 and profiles assume the classical log-linear forms.

The raised maximum can be a significant factor in the energy exchange process between the snow surface and the atmosphere. Instead of creating a stable atmosphere and retarding turbulent motions, the snow can transform the incoming solar radiation into a source of heat for the surface layer, not through convective motions, as other surfaces do, but through supplying moisture and reflected sunlight to the atmosphere. The heated atmosphere would then act as an elevated, almost blacktop surface in the presence of strong solar radiation causing unstable profiles and upward convection. Detailed knowledge of the temperature profile near the surface would be required in order to correctly estimate the sign and dimension of turbulent mixing. The warmed atmosphere would also radiate in the longwave allowing snow-melt to occur in the presence of a high albedo (>0.95 for fresh snow), weak winds, and a high emissivity (~0.99) in the longwave. It would also explain how the snow surface can sustain temperatures of 0°C in the presence of strong IR emission and inefficient conduction, which was not explained by Halberstam and Melendez (1979) whose model con-

sistently produced surface temperatures below 0°C. Granger and Male (1978), however, found that heat transfer to the snow is highly correlated with air temperatures at 85.0 kPa. This implies that the air mass temperature is more important in convective transfer than the temperature profile right above the surface. This could have significant implications for general circulation models, where poor resolution in the boundary layer has always been considered a hindrance in accurately computing fluxes. But if Granger and Male are correct, integrated air mass parameters may be more useful in assessing large-scale fluxes than local boundary-layer behavior. Certainly, snowmelt is an ideal means to evaluate the procedure because of its direct dependency on net heat flux from the atmosphere. Such a conclusion would also produce new applications for remote sounders of the atmosphere which supply integrated temperatures and humidities for the atmosphere.

Continued investigations of the surface layer over snow is expected. More data has recently been gathered with more and better equipment at a site near Pinedale, Wyoming. Weather conditions there were more varied and results should furnish a useful comparison with those described here.

Acknowledgments. The authors are extremely grateful to their colleagues at the Jet Propulsion Laboratory, Mssrs. W. Rachwitz and R. Machida, who labored extensively to render the equipment operational. They also thank Mr. J. F. Wickser, Northern District Engineer, Department of Water and Power, City of Los Angeles, and his colleagues at the Cane Ranch, Lee Vining, California for their assistance in the performance of this experiment. This paper presents the results of one phase of research carried out at the Jet Propulsion Laboratory, California Institute of Technology, under Contract NAS 7-100 sponsored by the Office of Weather and Climate, National Aeronautics and Space Administration.

REFERENCES

Anderson, Eric A., 1976: A point energy and mass balance mode of snow cover. NOAA Tech. Rep. N.W.S. 19, 150 pp.

Businger, J. A., 1973: Turbulent transfer in the atmospheric surface layer. *Workshop in Micrometeorology*, Amer. Meteor. Soc., 67–100.

——, J. C. Wyngaard, Y. Izumi, and E. F. Bradley, 1971: Flux-profile relationships in the atmospheric surface layers. *J. Atmos. Sci.*, **28,** 181–189.

De La Casaniere, A. C., 1974: Heat exchange over a melting snow surface. *J. Glaciol.*, **13,** 55–72.

Faraponova, G., V. Oppengeym, V. Kolesnikova, A. Mayorov and M. Kuznetsova, 1968: Determining the radiative flux in the lower layers of the atmosphere. *Atmos. Ocean. Phys.*, **4,** 950–959.

Geiger, R., 1965: *The Climate Near the Ground.* Harvard University Press (see pp. 93–102).

Granger, R. J., 1977: Energy exchange during melt of a prairie snowcover. MS thesis, University of Saskatchewan, 122 pp.

——, and D. H. Male, 1978: Melting of a prairie snowpack. *J. Appl. Meteor.*, **17,** 1833–1842.

Halberstam, I. M., and R. Melendez, 1979: A model of the planetary boundary layer over a snow surface. *Bound.-Layer Meteor.*, **16,** 431–452.

Kahle, A. B., J. Schieldge and H. Paley, 1977: JPL field measurements at the Finney County, Kansas test site, October 1976: Meteorological variables, surface reflectivity, surface and subsurface temperatures. JPL Publ. 77-1, 7–11.

Kondrat'yev, K. Ya., 1969: *Radiation in the Atmosphere.* Academic Press, 912 pp.

Kukla, G. J., and H. J. Kukla, 1974: Increased surface albedo in the Northern Hemisphere. *Science,* **183,** 709–714.

Lettau, H., 1957: Computation of Richardson numbers, classification of wind profiles, and determination of roughness parameters. *Exploring the Atmosphere's First Mile,* Vol. 2, Pergamon Press, 328–336.

McKay, D. C., and G. W. Thurtell, 1978: Measurements of the energy fluxes involved in the energy budget of a snow cover. *J. Appl. Meteor.*, **17,** 339–349.

Oke, T. R., 1970: The temperature-profile near the ground on calm, clear nights. *Quart. J. Roy. Meteor. Soc.*, **96,** 14–23.

Paulson, C., 1970: The mathematical representation of windspeed and temperature profiles in the unstable atmospheric surface layer. *J. Appl. Meteor.*, **6,** 857–861.

Schubert, J. F., 1977: Acoustic detection of momentum transfer during the abrupt transition from a laminar to a turbulent atmospheric boundary layer. *J. Appl. Meteor.*, **16,** 1292–1297.

Skibin, D., 1976: Uncoupled, vertically adjacent layers within the turbulent stable atmospheric layer. *Preprints Third Symp. Atmospheric Turbulence, Diffusion, and Air quality,* Raleigh, Amer. Meteor. Soc., 50–55.

Washington, W. M., and D. L. Williamson, 1977: A description of the NCAR global circulation models. *Methods in Computational Physics*, Vol. 17, J. Chang, Ed., Academic Press, 337 pp.

Wexler, H., 1936: Cooling in the lower atmosphere and the structure of polar continental air. *Mon. Wea. Rev.*, **64,** 122–136.

Zdunkowski, W., 1966: The nocturnal temperature minimum above the ground. *Beit. Phys. Atmos.*, **39,** 247–253.